Yuan *et al.*
Chinese Journal of Mechanical Engineering (2022) 35:73
https://doi.org/10.1186/s10033-022-00714-3

Chinese Journal of Mechanical Engineering

ORIGINAL ARTICLE

Open Access

Characteristics of Oscillation in Cavity of Helmholtz Nozzle Generating Self-excited Pulsed Waterjet

Miao Yuan[1,2], Deng Li[1,2*], Yong Kang[1,2], Hanqing Shi[1,2] and Haizeng Pan[1,2]

Abstract

Cavity flow oscillations in the axisymmetric cavity are critical to the operating efficiency of self-excited pulsed waterjets, which are widely employed in many practical applications. In this study, the behaviors of a turbulent flow in axisymmetric cavities causing cavity flow oscillations are investigated based on wall pressure characteristics. Experiments are performed using four Helmholtz nozzles with varying length-to-radius ratios at flow velocities of 20–80 m/s. Three orders of hydrodynamic modes in axisymmetric cavity are obtained through the spectral analysis of wall pressure. Based on the experimental results, the empirical coefficient of Rossiter's formula is modified, and the values of the parameter phase lag and the ratio of convection velocity to free stream velocity are obtained as 0.061 and 0.511, respectively. In addition, the spectral peak with a relatively constant frequency shows that the flow-acoustic resonance is excited significantly. A modified model is introduced based on the fluidic networks to predict the lock-on frequency. The results obtained can provide a basis for the structural optimization of the nozzle to improve the performance of self-excited pulsed waterjets.

Keywords: Self-excited cavitation waterjet, Flow-excited oscillations, Frequency characteristics, Vibration analysis

1 Introduction

Cavity flow oscillations caused by flows passing various cavities are typically observed in various industrial, aeronautical, energy, or marine applications [1–4], and they are an essential research object in the field of fluid mechanics [5]. Therefore, the cavity flow oscillations of water flows at moderate Reynolds number and air flows at high Mach numbers have been investigated extensively [6, 7]. Regarding experimental research pertaining to cavity flow oscillations caused by flows passing various cavities, primarily flow image display and flow measurement technology are typically prioritized. In terms of methods for measuring the dynamic pressure of walls, hot-wire experiments and particle image velocimetry are typically performed to measure the shear layer of the cavity and the flow in the cavity [8, 9].

Cavity flow oscillations caused by flows passing cavities are complicated and can be classified into either fluid-dynamic, fluid-resonant, or fluid-elastic oscillations [10]. In fluid-dynamic oscillations, two important elements must considered, i.e., the amplification of shear layer instability and the feedback mechanism, which can result in a cycle and the superposition of unstable oscillations in the cavity. Studies pertaining to cavity flow oscillations primarily focus on certain critical parameters, e.g., the Reynolds number or Mach number, thickness of the boundary layer, and ratio of the cavity length to cavity depth. In addition, the turbulence characteristics of flows are significant influencing factors in the cavity flow oscillations. Meganathan performed a visualization experiment on unsteady flows in a rectangular cavity characterized by their length-to-depth ratios (i.e., 2.5 and 3.3) under different flow velocities [11]. Different scales

*Correspondence: 2008lee@whu.edu.cn

[1] Hubei Key Laboratory of Waterjet Theory and New Technology, Wuhan University, Wuhan 430072, China
Full list of author information is available at the end of the article

of vortex structures in the shear layer can be observed in instantaneous images of flow fields, and they constantly coalesce to form larger vortexes in the downstream. By shifting up or down, the shear layer interacts with the collision wall of the cavity, thereby amplifying the unstable disturbance of the shear layer [12]. The vortex-edge interaction causes pressure to fluctuate on the wall, which is results in small-scale vortex shedding from the upstream shear layer [13].

By contrast, the primary reason for the pressure fluctuations caused by fluid-resonant oscillations is free-surface waves [10]. As shown in Figure 1, the structure of the cavity determines the direction of the acoustic standing wave. In a shallow cavity, a standing wave exists in the flow direction owing to the adequate cavity length. Hassan [14] investigated the flow oscillation of cavities under different flow velocities. Their results showed that oscillation occurred when the flow velocity exceeded a certain value, and that the frequency of flow oscillation induced by the cavity increased with the velocity. The cavity edge reflects the free-surface wave generated by the cavity, whereas excitations in the acoustic standing wave modes are determined by the cavity and wind tunnel geometry

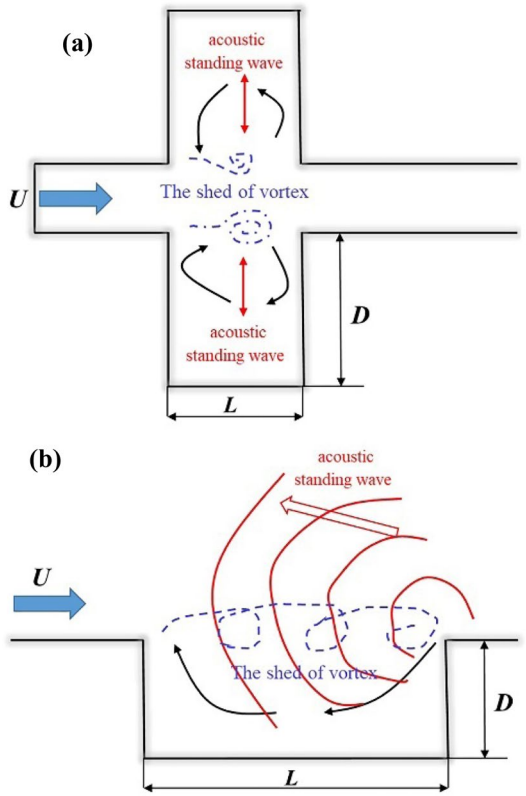

Figure 1 Schematic diagram of cavity flow oscillations: (**a**) deep cavity, (**b**) shallow cavity

under certain conditions, which causes pulsation and amplifies the pressure [15]. The spatial and temporal evolution of the vortex structure is accompanied by the acoustic mode of the cavity. The energy input of the flow field enhances the acoustic wave, whereas the high amplitude acoustic wave excites the evolution of the vortex structure, thereby generating flow in the cavity and hence displaying the characteristics of self-sustaining oscillations [16].

Cavity flow oscillations are typically considered unfavorable for fluid machinery systems; this is because significant oscillations can result in noise, vibration, considerable decline in efficiency, material damage, cavitation, and performance deteriorations. However, cavity flow oscillations are crucial in improving drilling and cutting efficiency as well as in enhancing the effect of surface treatment [17–20]. Morel investigated self-excited cavitation waterjets induced by a gas jet through an axisymmetric cavity, as shown in Figure 1, and discovered that self-resonating oscillations involved three mechanisms. The first mechanism pertains to the instability of the jet shear layer and its amplification, the second is the cavity resonance, and the third is the periodic feedback interference of the collision shear layer [21]. In such configurations, energetic vortices shed from the upstream nozzle and formed at the self-resonating cavity are coupled closely with the natural modes of the nozzle; additionally, sustained standing waves are established in a positive feedback mechanism. By amplifying the unsteady disturbance, the self-sustained oscillating nozzle generates periodic disturbance in the upstream through the feedback of shear layer instability to form self-sustained oscillating jets. Based on such a principle, the oscillating jet issued from the Helmholtz nozzles was applied in water jet engineering to improve the operating efficiency of water jets [17, 22–24].

In recent years, the development of self-excited cavitation waterjets have progressed rapidly in various industrial applications, e.g., cutting, mining, materials processing, and heat transfer. Using the Helmholtz nozzle to generate self-sustained oscillating SC-CO 2 jets, Huang et al. investigated the effect of self-sustained oscillations on the characteristics of jet erosion [25]. The experimental results showed that self-sustaining oscillations can significantly increase the peak pressure and erosion capacity of the jet, which is conducive to extending the application of jets in oil and gas exploration. Ding et al. applied self-excited oscillating jets for material surface treatment and achieved significant progress [26]. Fan et al. proposed a nozzle comprising two parallel chambers and obtained the natural frequency of the nozzle through deduction [27]. The results showed that the frequency of self-excited oscillations decreased as

the length-to-depth ratios of the two parallel chambers increased.

The use of axisymmetric cavity shown in Figure 2 to induce self-excited cavitation oscillation jets is an important application based on this principle in water jet engineering and is effective in significantly improving the operating efficiency of water jets. Despite the simple structure of the axisymmetric cavity, the characteristics of flows past the cavity are complex, and the interaction between the fluid and cavity is not elucidated. A significant factor in improving the operating efficiency of self-excited cavitation waterjets is the moderate relationship between the flow condition and the cavity geometry. Experimental studies regarding flow characteristics in axisymmetric cavities are crucial for solving this problem.

In this study, the oscillation coupling between a standing sound wave and the hydrodynamic oscillation in the context of the axisymmetric cavity was investigated. First, the formulation of experimental facilities and methodologies are introduced; four different configurations of axisymmetric cavities were used in this study. Subsequently, the oscillation coupling between the standing sound wave and the hydrodynamic oscillation in axisymmetric cavity is discussed. Second, a preliminary theoretical analysis of hydrodynamic oscillation and acoustic modes was conducted. Third, the effect of geometry resonance modes on the operating ability of self-excited cavitation waterjets was investigated based on the increment in pressure as measured at the four nozzles' outlet. Finally, conclusions regarding cavity flow oscillations in an axisymmetric cavity are presented.

2 Experimental Setup and Procedures

2.1 Experimental Setup

An experimental investigation was conducted using a multifunction waterjet test bench, which was developed independently by Hubei Key Laboratory of Waterjet Theory and New Technology and had been used for several investigations previously [17, 23]. The experimental flowchart of the cavity flow oscillations tests is illustrated in Figure 3.

The multifunction waterjet test bench can achieve a high pressure water stream pressure of up to 60 MPa, which causes the speed of the free stream flow to vary in the test section. The nozzle was connected to the pump via the pipeline. A high-frequency pressure transducer (model: HELM91) mounted onto the nozzle wall was used as the test section to investigate the pressure fluctuation at the nozzle walls. Transducers with a diameter of 6 mm were connected to the interior of the cavity through 1-mm-diameter pinholes and a threaded hole, which can reduce the nozzle effects on the flow conditions inside the nozzle. Significant differences in Pressure fluctuations were not observed in the experimental results [16, 28]; hence, it can be inferred that the presence of the high-frequency pressure transducer inside the nozzle with the abovementioned flow conditions does not significantly affect the flow.

Combined with theoretical calculation and experimental results [29–31], four nozzles with different inner diameters were employed in the experiment, and the specifications of the nozzle are shown in Table 1. The pressure signals were received by the data logger (model: HBM Quantum X MX840B-8) at a 19200 Hz sample rate. In this case, the pressure signals were bandpass filtered by the signal conditioner. The operating frequency of the motor was regulated continuously to obtain different pump pressures.

The flow velocity in the tested section was measured using a turbine flowmeter installed at the pump outlet. For each experiment, the flow velocity at the test section ranged from 20 to 80 m/s. Owing to the unique operating

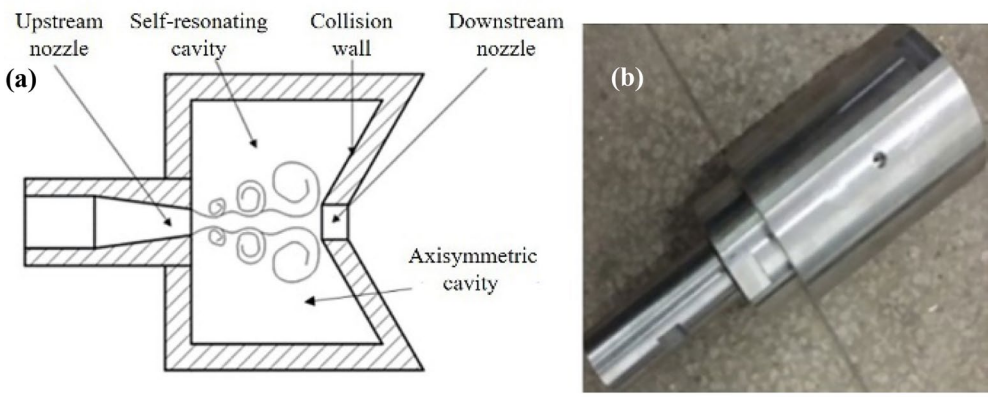

Figure 2 Schematic diagram (**a**) and photograph (**b**) of 120°-impinging edge Helmholtz nozzle

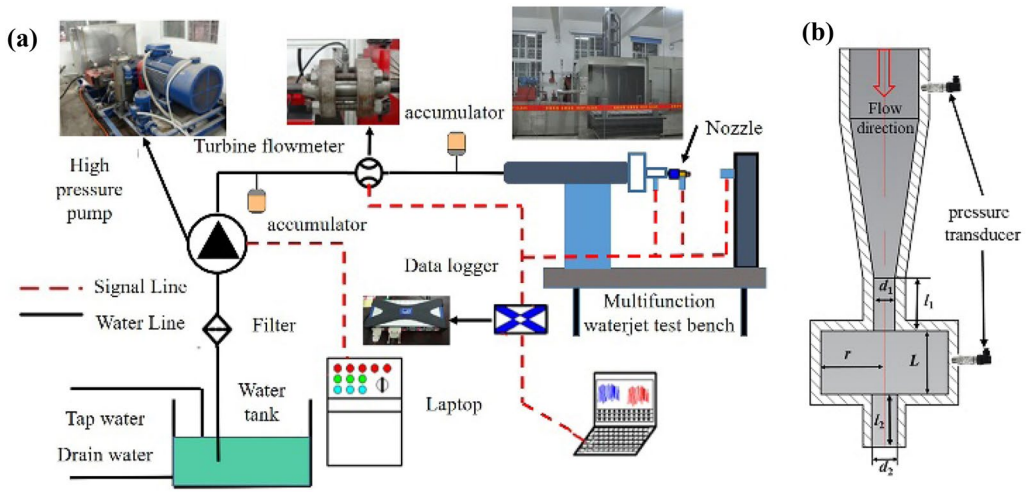

Figure 3 Schematic diagram of experimental setup: (**a**) experimental system, (**b**) tested section

Table 1 Specifications of upstream nozzle

	Inlet diameter d_1 (mm)	Inlet length l_1 (mm)	Cavity radius r (mm)	Cavity length l (mm)	Inlet diameter d_2 (mm)	Outlet length l_2 (mm)
Case 1	2	5	24	12	2.4	2
Case 2	2	5	12	12	2.4	2
Case 3	2	5	12	24	2.4	2
Case 4	2	5	12	48	2.4	2

principle of the plunger pump during the pump strokes, the initial pressure fluctuated in the experimental system. To capture the cavity flow oscillations in real time, the perturbations caused by the pump must be minimized. More specifically, two bladder accumulators were placed in the pipeline, near the pump and nozzle, separately.

2.2 Experiment Uncertainty

For the entire system, the main experiment uncertainty was the accuracy of the pressure transducer and the reliability of the turbine flowmeter, which were less than 0.1% FS, ±0.5% FS, respectively. The total uncertainty of the experimental system as calculated using uncertainty propagation theory was ±0.51% FS.

3 Experimental Results

3.1 Spectral Analysis of Pressure Data

To provide a global view of the cavity flow oscillations for different cavities, the power spectra of pressure fluctuations inside each cavity are shown in Figure 4. For each spectrogram, the flow velocity at the tested section ranged from 20 to 80 m/s, and a total of 61 spectra from an average of 10 experiments are shown simultaneously. Different numbers of spectral peaks were observed in the spectrogram, which clearly indicates that the frequency and amplitude of the oscillation are associated with the velocity.

For each pressure spectrogram measured at the wall of the four cavities, three linear lines were highlighted; they showed that the frequency of the cavity flow oscillations increased slowly as the velocity increased, and that three orders of the hydrodynamic oscillation modes occurred in the cavity within this velocity range. The order number n of the hydrodynamic mode represents the number of vortices in the shear layer [32].

Additionally, a spectral peak with a relatively constant frequency is shown in Figure 4b–d, which is different from the hydrodynamic modes excited by the instability of the shear layer. It was assumed that the spectral peak characterized the flow-tone lock-on phenomenon, or flow-acoustic resonance [33]. During the flow-acoustic resonance, a sufficiently high amplitude of pressure oscillations above the background pressure was identified, where the peak amplitudes of the pressure oscillation reached 138 dB. As for the oscillation peak with a significant amplitude, it was discovered that the frequency of

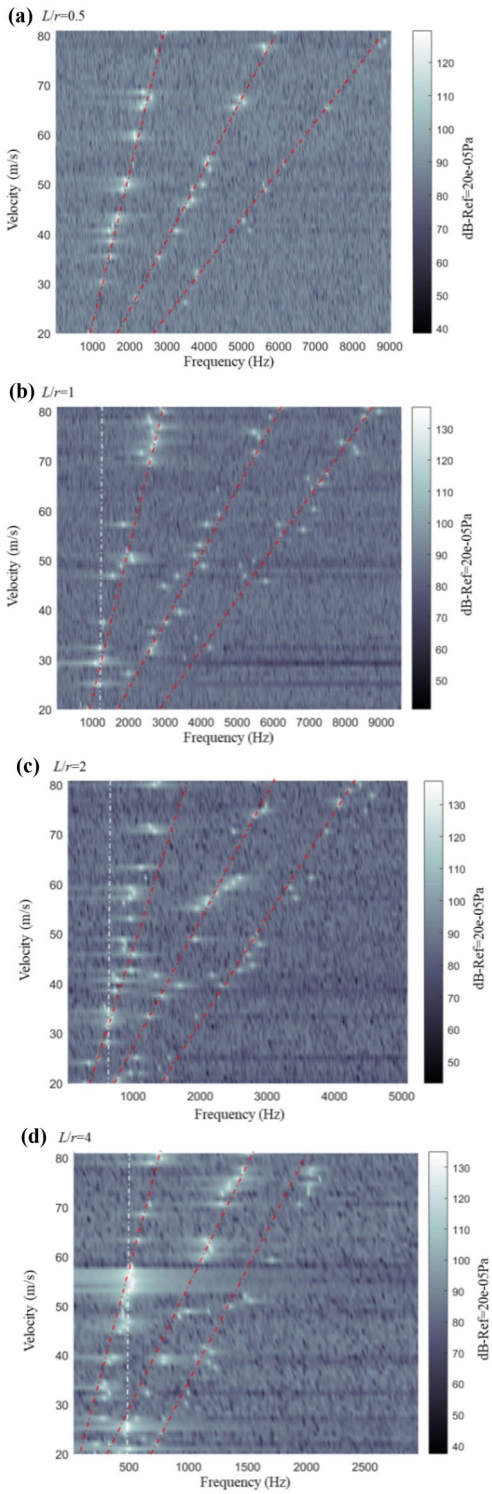

Figure 4 Speed-dependent spectrogram measured at cavity wall

the hydrodynamic oscillation mode was comparable to that of the geometry resonance modes.

3.2 Frequency Characteristic of Cavity Flow Oscillations

To analyze the statistical characteristics of the hydrodynamic and geometry resonance modes for wall pressure oscillation, the frequency of the localized peaks was plotted, as shown in Figure 5. The figure shows that the frequency of geometry resonance modes induced by different conditions barely changed, and that the fitting lines of the three orders of hydrodynamic modes reflected the particular frequency range.

As shown in Figure 4, the oscillation amplitudes of the hydrodynamic modes were smaller than the amplitudes of the lock-on frequency. As the velocity increased, the frequency of each order hydrodynamic mode increased accordingly. Meanwhile, frequency coincidence occurred between the geometry resonance modes and the second- or first-order hydrodynamic mode. As the velocity increased from 20 to 80 m/s, frequency lock-on was observed, and the number of frequency lock-on was 0, 1, 1, and 2 for the different axisymmetric cavities, separately.

In addition, the cavity length affects the occurrence of pressure oscillation. In general, the oscillation frequency in the hydrodynamic mode and the frequency of the geometry resonance modes are negatively correlated with the cavity length, which is consistent with Figure 5.

If the flow velocity is constant, then the oscillation frequency of the shear layer barely changes, whereas the resonance frequency of the standing wave is reduced when the cavity length is increased. As shown in Figure 5a, however, the characteristics of the frequency lock-on were beyond recognition, which indicates that the instability of the shear layer dominated the pressure oscillation in the cavity.

The oscillation was reinforced by the interaction between the geometry resonance modes and the appropriate hydrodynamic mode, which is the essence of frequency coincidence. Compared with the frequency of the geometry resonance modes, these high-intensity frequencies indicate a less significant error, suggesting that the natural acoustic standing waves inside amplify the pressure fluctuation [34].

Additionally, with regard to amplitude, the local maximum in the pressure amplitude spectrum suggests the coupling between the acoustic standing waves and the shear layer [8]. Notably, the resonance amplitude of the lock-on frequency was approximately one order of

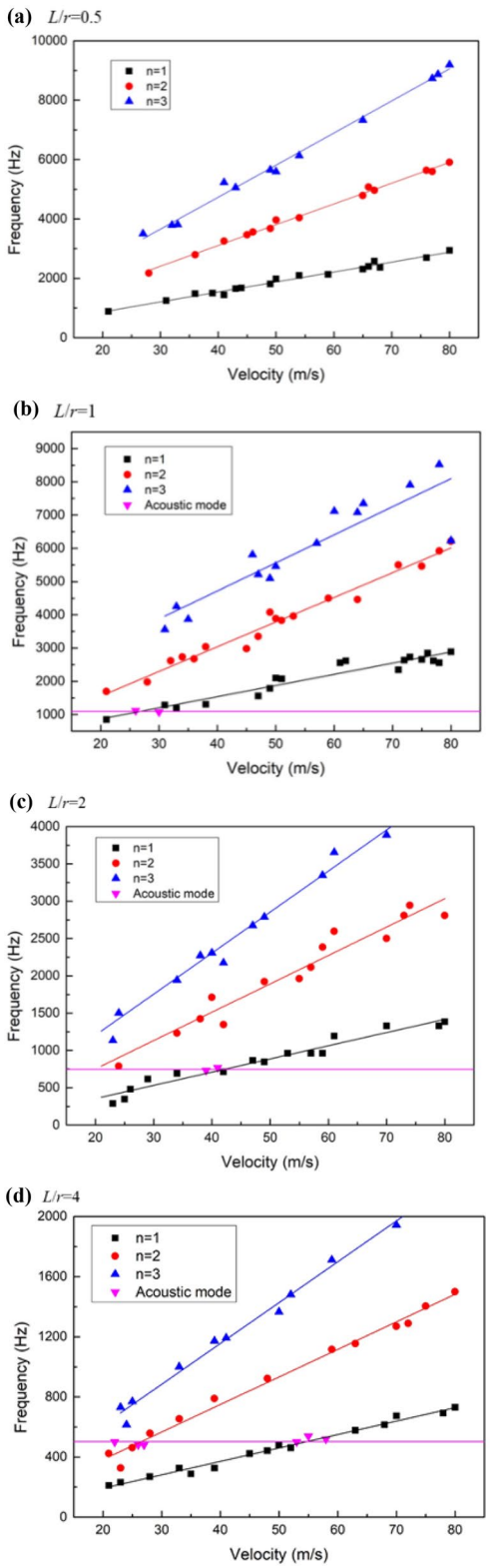

Figure 5 Frequency of cavity pressure oscillation as a function of free stream velocity

magnitude higher than the pressure fluctuation in the hydrodynamic mode. This highlights the capacity potential of self-excited cavitation waterjets in various industrial applications.

3.3 Modified of Empirical Coefficient in Rossiter's Formula

In the self-excited cavitation waterjet issued from the Helmholtz nozzles, a shear layer was formed at the mouth of the cavity owing to momentum exchange. Subsequently, vortex rings were induced by the fluids entrained into the shear layer. After shedding from the anterior edge of the cavity, the vortex ring was enlarged continuously and became less stable gradually until the downstream edge was affected. Subsequently, the pressure wave propagated forward to the front wall, further aggravating the instability of the shear layer and generating a new vortex ring in the cavity. Oscillation occurred in the shear layer when the pressure wave formed an effective periodic feedback.

Pressure fluctuation characterizes the oscillations resulting from the interaction of the shear layer instability and the intracavitary flow. Rossiter constructed a simple model to obtain a formula for calculating the non-dimensional frequency of oscillations, as follows [35]:

$$S_{tr} = \frac{fL}{U_\infty} = \frac{n-\alpha}{M_\infty + 1/\kappa_v}, \tag{1}$$

where S_{tr} represents the Strouhal number of oscillations; M_∞ and L indicate Mach Numbers of the flow and cavity lengths, respectively; n denotes the number of shear layer hydrodynamic modes; α and κ_v refer to the phase lag and ratio of convection velocity to free stream velocity, respectively, whose values in this study were 0.25 and 0.57, respectively.

Compared with our experimental results, the frequency of the hydrodynamic mode calculated using Eq. (1) and the frequency of the pressure oscillation differed, which is primarily attributed to the mismatch between different empirical coefficients. Therefore, the parameter phase lag and the ratio of the convection velocity to the free stream velocity must be adjusted to fit the pressure data when using the Rossiter formula developed for the cavity flow oscillations of water; this is to accommodate the difference in compressibility and wave velocity between water and air. Owing to the intense momentum exchange, cavitation occurred in the cavity, and the characteristics of the mixture flow changed. By fitting the data captured in cavity flow oscillations experiments of water, the values of the parameter phase lag and the ratio of the convection velocity to the free stream velocity at different Mach Numbers were calculated and shown in Table 2. Then the average values of α and κ_v of 0.061 and 0.511 were obtained, respectively.

Table 2 Least-squares fitting values of empirical coefficients

M_∞	S_{tr1}	S_{tr2}	S_{tr3}	α	κ_v
0.14386	0.472308	0.951601	1.53157	0.109	0.574
0.17193	0.442878	0.89989	1.38517	0.063	0.514
0.175439	0.475575	0.95115	1.343615	0.001	0.497
0.189474	0.465999	0.897796	1.363794	0.004	0.499
0.22807	0.426206	0.884378	1.353205	0.081	0.519
0.280702	0.441523	0.885932	1.379399	0.06	0.541
0.17193	0.423817	0.993883	1.248544	0.001	0.458
0.175439	0.503279	0.932681	1.311295	0.001	0.497
0.273684	0.393649	0.911608	1.311176	0.143	0.526
0.280702	0.433287	0.93221	1.23499	0.001	0.467
0.119298	0.488884	0.869126	1.37159	0.004	0.485
0.147368	0.406756	0.769539	1.242256	0.027	0.446
0.17193	0.414609	0.942293	1.366324	0.128	0.519
0.207018	0.391291	0.930402	1.341693	0.177	0.528
0.214035	0.469293	1.021847	1.438155	0.03	0.541
0.245614	0.455127	0.857486	1.332402	0.004	0.5
0.280702	0.415551	0.842645	1.292826	0.053	0.501
0.080702	0.483388	0.682548	1.525695	0.074	0.545
0.115789	0.475715	0.95143	1.455128	0.029	0.52
0.136842	0.422528	0.930803	1.414366	0.149	0.533
0.245614	0.395723	0.870679	1.332402	0.155	0.53
Average value				0.061	0.511

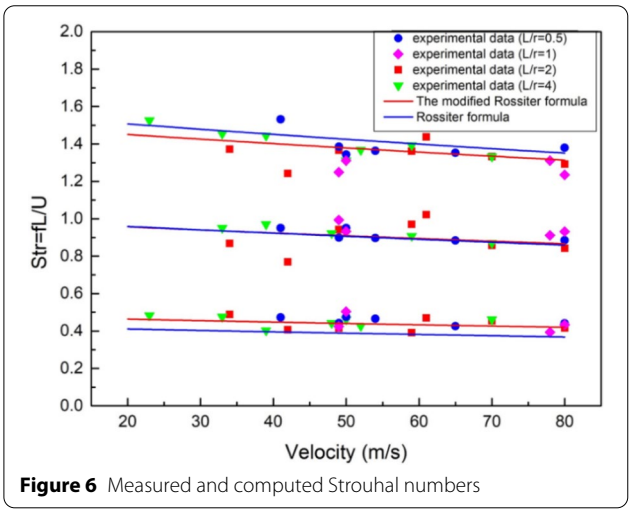

Figure 6 Measured and computed Strouhal numbers

Figure 6 shows the variation in the Strouhal numbers under three orders of hydrodynamic modes as a function of the free stream velocity. The Rossiter formula combined with two modified parameters is plotted for comparison. As shown in Figure 6, the Rossiter formula fitted smoothly to the experimental data for most of the conditions after the empirical coefficients were modified.

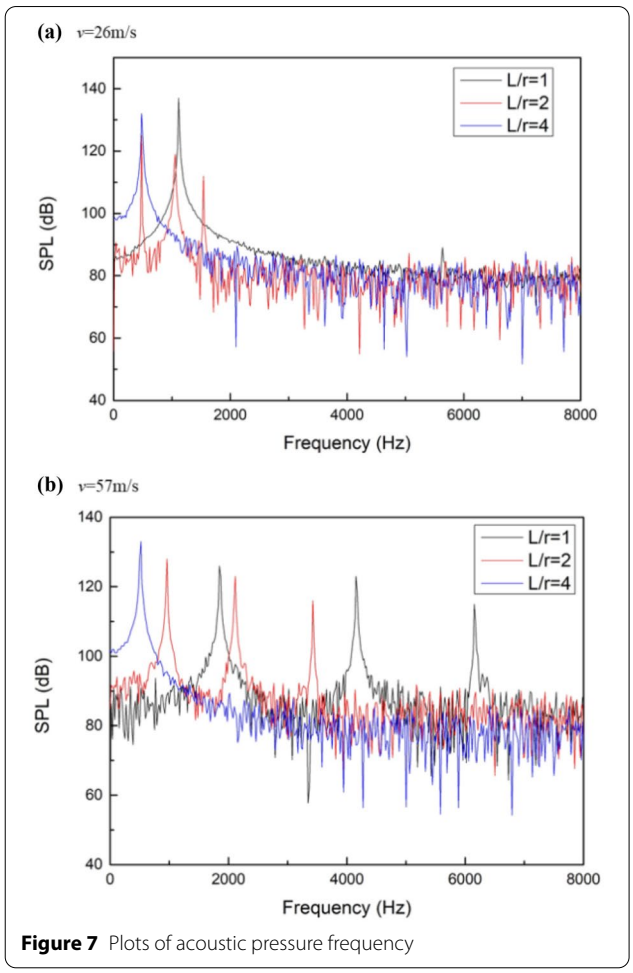

Figure 7 Plots of acoustic pressure frequency

4 Discussion of Flow-Acoustic Resonance

4.1 Characteristics of Flow-Acoustic Resonance

The spectrum power of wall pressure for $V_{\text{in}} = 26$ and 57 m/s was obtained to characterize the frequency of the pressure oscillation, as shown in Figure 7. The sound pressure level (SPL) is defined as follows:

$$SPL\,(\text{dB}) = 20 \cdot \log_{10}\left(\frac{\overline{p}}{p_{ref}}\right). \tag{2}$$

The pressure responses of the axisymmetric cavity show a number of additional features. First, the coupling of acoustic standing waves and the shear layer occurred under specific flow conditions. The oscillation frequency of the hydrodynamic modes was a function of velocity, and a specific range of Strouhal numbers was identified, in which the frequency of the hydrodynamic

modes coincided with the geometry resonance modes and contributed to the flow-acoustic resonance. When the length-to-radius ratio (L/r) reached 4, the frequency of the second-order hydrodynamic mode close to the frequency of the geometry resonance modes and flow-tone lock-on frequency were indicated at a velocity was 26 m/s. When the cavity length changed and L/r was 2, the two oscillations were decoupled and the third-order hydrodynamic mode dominated the pressure oscillation. Furthermore, the first-order hydrodynamic mode excited the geometry resonance modes. At the velocity of 57 m/s, however, flow-tone lock-on occurred only when the cavity length was four times the radius.

The second feature refers to the order of the hydrodynamic modes that couples with the geometry resonance modes. As shown in Figure 7a, the flow-acoustic resonance occurred in the pressure spectrum of the cavity wall with $L/r = 1$ and 4. The frequency and amplitude of the flow-acoustic resonance differed for the two test sections. When L/r was 4, the geometry resonance modes was excited by the second-order hydrodynamic mode. Additionally, its amplitude was lower compared with those of the geometry resonance modes when L/r was 1.

In general, as the length of cavity varied, the first-order hydrodynamic mode interacted with the natural acoustic standing waves, with most of the energy concentrated in the resonance modes. In other words, the oscillation pressure at the cavity wall enhanced when the frequency of the hydrodynamic modes was similar to the resonant frequency of standing waves, which results in coupling resonance. In this case, however, the energy in the other hydrodynamic modes diminishes or disappears.

Furthermore, the coupling resonance of the same standing wave resonance in the lower hydrodynamic mode is stronger than that under a higher hydrodynamic mode. The energy of pressure oscillation focuses on a fundamental frequency, whereas the other hydrodynamic mode reduces or attenuates. Hence, it is speculated that the frequency of the hydrodynamic mode is higher than those of the geometry resonance modes in the tested velocity range; additionally, only when the shear layer instability excites the geometry resonance modes can flow-acoustic resonance occur.

4.2 Frequency Prediction of Geometry Resonance Modes

The frequency of the geometry resonance modes is determined by the cavity structure. Generated in a fluid system, standing waves cause pressure to fluctuate through resonance wave effects, which are defined by the geometry of the fluid system and the boundary conditions. However, the standing waves in the cavity tend to interact with the shedding vortex, which causes more significant pressure fluctuations. Consequently, the mechanism of pressure oscillation in the cavity is complicated. Hence, the analogy of fluid networks with cavity flow oscillations within the cavity is proposed herein to investigate the geometry resonance modes of the fluid system. Liu et al. simulated a self-excited inspiratory jet to a *LC* electrical circuit, where two basic analogous quantities of mass flow Q_M and fluidic potential P were defined, which is consistent with the principles of current and voltage [17]. Therefore, the relationships based on the continuity equation and the analogy of mechanical power are as follows:

$$\sum Q_M = 0, \tag{3}$$

$$P \approx \int \frac{\mathrm{d}p}{\rho} + \frac{u^2}{2} = \frac{p^*}{\overline{p}}\left(p^* + \overline{p}\frac{u^2}{2}\right). \tag{4}$$

Meanwhile, the three basic analogous elements, including the fluidic resistance, fluidic inductance, and fluidic capacitance, are defined as follows:

$$R = \frac{\Delta P}{Q} = \frac{128\mu l}{\pi D^4 \rho}, \tag{5}$$

$$L = \frac{\Delta P}{\mathrm{d}Q/\mathrm{d}t} = \frac{l}{A}, \tag{6}$$

$$C = \frac{\int Q\mathrm{d}t}{\Delta P} = \frac{V}{a^2}. \tag{7}$$

For the fluid system investigated in this study, the effect of the downstream pipe must be considered. The equivalent circuit of the fluid system used in this study is shown in Figure 8, from which it is clear that it is similar to the equivalent circuit of a Helmholtz oscillator. However, the significant difference between them is the presence of fluidic resistance and fluidic inductance in parallel with the fluidic capacitance, which changes the overall impedance of the fluid system.

Based on the corresponding equivalent circuit diagram, the flow and pressure can be expressed as follows:

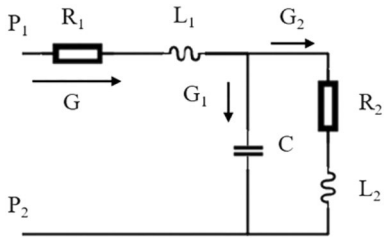

Figure 8 Analogical *LC* electrical circuit diagram

$$G = G_1 + G_2, \tag{8}$$

$$P_1 - P_2 = GR_1 + L_1\frac{\mathrm{d}G}{\mathrm{d}t} + G_2R_2 + L_1\frac{\mathrm{d}G_2}{\mathrm{d}t}, \tag{9}$$

$$\frac{1}{C}\int G_1\mathrm{d}t = G_2R_2 + L_2\frac{\mathrm{d}G_2}{\mathrm{d}t}. \tag{10}$$

Hence, the total impedance of the fluid system is

$$\begin{aligned} Z &= R_1 + j\omega L_1 + \frac{\frac{1}{j\omega C}(R_2 + j\omega L_2)}{R_2 + j\omega L_2 + \frac{1}{j\omega C}} \\ &= R_1 + \frac{R_2}{\omega^2C^2R_2^2 + \left(1 - \omega^2L_2C\right)^2} \\ &\quad + j\omega\left[L_1 + \frac{L_2 - \omega_2L_2C - R_2^2C}{\omega^2C^2R_2^2 + \left(1 - \omega^2L_2C\right)^2}\right]. \end{aligned} \tag{11}$$

Resonance occurs when the imaginary component of the impedance is zero:

$$L_1 + \frac{L_2 - \omega_2L_2C - R_2^2C}{\omega^2C^2R_2^2 + \left(1 - \omega^2L_2C\right)^2} = 0. \tag{12}$$

Hence, the resonant frequency is calculated as follows:

$$\omega = \sqrt{\frac{2L_1L_2 + L_2^2 - L_1CR_2^2 \pm \sqrt{L_1CR_2^4 - 4L_1^2L_2CR_2^2 + 2L_1L_2^2CR_2^2 + L_2^4}}{2L_1L_2^2C}}, \tag{13}$$

$$f = \frac{1}{2\pi}\sqrt{\frac{2L_1L_2 + L_2^2 - L_1CR_2^2 \pm \sqrt{L_1CR_2^4 - 4L_1^2L_2CR_2^2 + 2L_1L_2^2CR_2^2 + L_2^4}}{2L_1L_2^2C}}. \tag{14}$$

Intuitively, the frequency of the geometry resonance modes is associated with not only the structure of the fluid system, but also the wave velocity of water. Additionally, cavitation occurs in the cavity owing to the unique structure of the axisymmetric cavity, which results in a rapid decline in the wave velocity of water.

Table 3 Predicted frequency of geometry resonance modes

Test case	Frequency (Hz)	Wave velocity *a* (m/s)
1	523	285
2	1047	
3	740	
4	523	

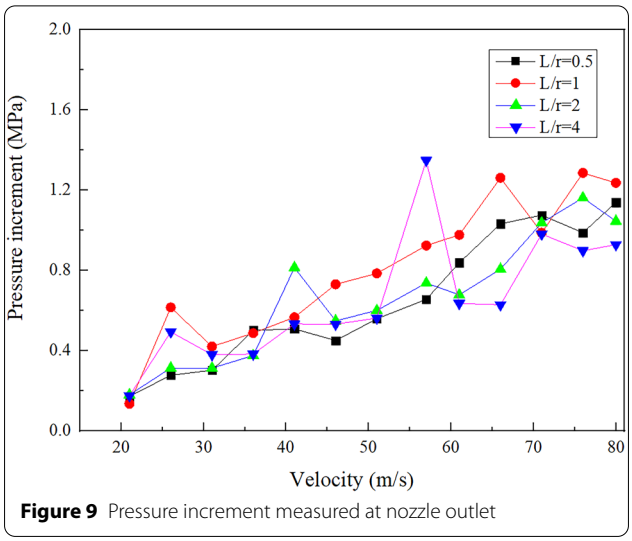

Figure 9 Pressure increment measured at nozzle outlet

The intrinsic frequency for the different sizes of the test section is indicated in Table 3.

In summary, the average frequencies of the flow-acoustic resonance were 503, 745, and 1096 Hz for tests 4, 3, and 2, respectively, which are consistent with the fluidic model of frequency prediction. However, the hydrodynamic mode coupled with the geometry resonance modes in a certain frequency range, owing to the effect of cavitation. In a cavity, periodic cavitation structures tend to change the wave velocity and modulate the couple relationship between the hydrodynamic mode and geometry resonance modes.

4.3 Effect of Flow-Acoustic Resonance on Self-Excited Cavitation Waterjet

Self-excited cavitation waterjets impose a periodical effect on the target through intense pressure oscillations produced by cavity flow oscillations. Therefore, the destructive ability is considerably more significant compared with that of a continuous jet; consequently, the erosion ability and operating efficiency of the target material are improved significantly.

Pressure increment is an important parameter for assessing the operating ability of self-excited cavitation waterjets. The pressure increment measured at the four nozzles' outlet were plotted, as shown in Figure 9. An increase in the amplitude of the outlet pressure caused partially by cavity flow oscillations was observed. Furthermore, it was discovered that the pressure increment was associated with the cavity length, and that it reached a maximum value when L/r was 1, which is consistent with the intensity of cavity flow oscillations in the cavity. When $L/r = 1$, the instability of the shear layer resulted in cavity flow oscillations, resulting in a higher pressure.

Furthermore, it is noteworthy that significant peaks were observed when $L/r = 1$, 2, and 4. As shown in Figure 9, the significant peak was associated with the flow-acoustic resonance at $V_{\text{in}} = 26$ and 41 m/s, in which the first-order hydrodynamic modes excited the geometry resonance modes. Similarly, frequency lock-on was observed at the two inlet velocities for $L/r = 4$. However, at $V_{\text{in}} = 26$ and 41 m/s, the geometry resonance modes were caused by the second- and first-order hydrodynamic modes, respectively. The pressure increment was consistent with the amplitude of the coupling resonance, which was attributed to the intensity of the hydrodynamic modes that resulted in the geometry resonance modes.

5 Conclusions

Pressure oscillations in an axisymmetric cavity are significantly associated with the mechanism of self-excited cavitation waterjets. In this study, the cavity flow oscillations of self-excited cavitation waterjets caused by an axisymmetric cavity were investigated. The pressure oscillation of the jet and the wall pressure of the axisymmetric cavity were investigated both experimentally and analytically. Because it was difficult to measure the volume fraction of vapor caused by intense cavitation, a standard value for the wave velocity and a frequency range for geometry resonance modes could not be obtained theoretically. However, the conclusions obtained in this study can provide a basis for the structural optimization of the nozzle to improve the performance of self-excited cavitation waterjets. The conclusions are as follows:

(1) In the self-excited cavitation waterjet issued from the axisymmetric cavity, the oscillations of the shear layer corresponded to three orders of hydrodynamic modes. By fitting the experimental data, Rossiter's formula was modified to render it more suitable for low Mach numbers in water. The value of the parameter phase lag and the ratio of the convection velocity to the free stream velocity was determined to be 0.061 and 0.511, respectively.

(2) The spectral analysis of the wall pressure revealed the occurrence of flow-acoustic resonance under certain flow conditions. When flow-acoustic resonance occurred, a sufficiently high-pressure amplitude above the background pressure was observed, and the peak amplitudes of the pressure oscillation reached up to 138 dB.

(3) Based on fluidic networks, a modified model was proposed to predict the lock-on frequency. Standing waves were generated in a fluid system to generate pressure fluctuations through resonance wave effects, which are defined by the geometry of the fluid system and the boundary conditions. Flow-acoustic resonance occurred when the standing waves in the cavity interacted with the shedding vortex, which then resulted in more significant oscillations.

(4) The length of the axisymmetric cavity was associated with the performance of the self-excited cavitation waterjet. For the four Helmholtz nozzles, the amplitude of the pressure oscillation reached its maximum gradually as the cavity length was reduced; the maximum pressure oscillation for the self-excited cavitation waterjet occurred when $L/r = 1$. In addition, the pressure oscillation of the self-excited cavitation waterjet doubled because the flow-acoustic resonance occurred under specific flow conditions.

Acknowledgements
Not applicable.

Authors' Information
Miao Yuan, born in 1996, is currently a PhD candidate at *Hubei Key Laboratory of Waterjet Theory and New Technology, Wuhan University, China*. His research interests include Self-excited Pulsed Waterjet.
Deng Li, born in 1987, is currently an associate professor at *Wuhan University, China*. He received his doctor degree in *Wuhan University, China*, in 2017.
Yong Kang born in 1978, is currently a professor at *School of Power and Mechanical Engineering, Wuhan University,China*. He received his PhD degree from ChongQing University, China, in 2006. His research interests include waterjet theory and supercritical carbon dioxide jet technology.
Hanqing Shi is currently a PhD candidate at *School of Power and Mechanical Engineering, Wuhan University, China*.
Haizeng Pan is currently a PhD candidate at *School of Power and Mechanical Engineering, Wuhan University, China*.

Author Contributions
MY: formal analysis, investigation, writing - original draft. DL: investigation and writing. YK: supervision and funding acquisition. HS and HP: experiment. All authors read and approved the final manuscript.

Funding
Supported by National Natural Science Foundation of China (Grant Nos. 52175245, 51805188), Fundamental Research Funds for the Central Universities of China (Grant No. 2042020kf0001), and National Key Research and Development Program of China (Grant No. 2018YFC0808401).

Competing Interests
The authors declare no competing financial interests.

Author Details
[1]Hubei Key Laboratory of Waterjet Theory and New Technology, Wuhan University, Wuhan 430072, China. [2]School of Power and Mechanical Engineering, Wuhan University, Wuhan 430072, China.

Received: 4 November 2020 Revised: 8 October 2021 Accepted: 29 March 2022
Published online: 11 June 2022

References

[1] Deng Li, Yong Kang, Xiaolong Ding, et al. Effects of area discontinuity at nozzle inlet on the characteristics of self-resonating cavitating waterjet. *Chinese Journal of Mechanical Engineering*, 2016, 29(4): 1-12.
[2] G Loupy, G Barakos, N Taylor. Cavity flow over a transonic weapons bay during door operation. *Journal of Aircraft*, 2017: 1-16.
[3] DWlabc, K Yong, C Xwab, et al. Integrated CFD-aided theoretical demonstration of cavitation modulation in self-sustained oscillating jets. *Applied Mathematical Modelling*, 2020, 79: 521-543.
[4] Peng Wang, Hongyu Ma, Yifan Deng, et al. Influence of vortex-excited acoustic resonance on flow dynamics in channel with coaxial side-branches. *Physics of Fluids*, 2018, 30(9).
[5] K M Nair, S Sarkar. Large eddy simulation of self-sustained cavity oscillation for subsonic and supersonic flows. *Journal of Fluids Engineering*, 2016, 139(1).
[6] J Basley, L R Pastur, F Lusseyran, et al. Experimental investigation of global structures in an incompressible cavity flow using time-resolved PIV. *Experiments in Fluids*, 2011, 50(4): 905-918.
[7] G M Di Ciccaa, M Martinezb, C Haigermoser, et al. Three-dimensional flow features in a nominally two-dimensional rectangular cavity. *Physics of Fluids*, 2013, 25: 7101.
[8] P Oshkai, M Geveci, D Rockwell, et al. Imaging of acoustically coupled oscillations due to flow past a shallow cavity: Effect of cavity length scale. *Journal of Fluids & Structures*, 2005, 20(2): 277–308.
[9] L Ukeiley, N Murray. Velocity and surface pressure measurements in an open cavity. *Experiments in Fluids*, 2005, 38(5): 656-671.
[10] D Rockwell, E Naudascher. Review—Self-sustaining oscillations of flow past cavities. *ASME Transactions-Journal of Fluids Engineering*, 1978, 116: 157-186.
[11] A Vakili, A Meganathan. Effect of upstream mass-injection on cavity flow oscillations (PIV measurements compared with CFD predictions). *Aerospace Sciences Meeting & Exhibit*, 2003.
[12] C H Kuo, S H Huang, C W Chang. Self-sustained oscillation induced by horizontal cover plate above cavity. *Journal of Fluids & Structures*, 2000, 14(1): 25-48.
[13] A Meganathan, A Vakili. An experimental study of open cavity flows at low subsonic speeds. *40th AIAA Aerospace Sciences Meeting & Exhibit*, 2002.
[14] M E Hassan, L Labraga, L Keirsbulck. *Aero-acoustic oscillations inside large deep cavities*. The University of Queensland, 2007.
[15] O McGregor, R White. Drag of rectangular cavities in supersonic and transonic flow including the effects of cavity resonance. *AIAA Journal*, 1970, 8: 1959-1964.
[16] Youjun Zhu, Hua Ouyang, Z Du. Experimental investigation of acoustic oscillations over cavities. *Proceedings of the Institution of Mechanical Engineers, Part G: Journal of Aerospace Engineering*, 2010, 224: 697-704.
[17[W Liu, Y Kang, M Zhang, et al. Experimental and theoretical analysis on chamber pressure of a self-resonating cavitation waterjet. *Ocean Engineering*, 2018, 151: 33-45.
[18] Deng Li, Yong Kang, Xiaolong Ding, et al. Experimental study on the effects of feeding pipe diameter on the cavitation erosion performance of self-resonating cavitating waterjet. *Experimental Thermal and Fluid Science*, 2017, 82: 314-325.
[19] V E Johnson, W T Lindenmuth, A F Conn, et al. Feasibility study of tuned-resonator, pulsating cavitating water jet for deep-hole drilling. *Petroleum*, 1981.
[20] G L Chahine, K M Kalumuck, G S Frederick. The use of self resonating cavitating water jets for rock cutting. *8th American WaterJet Conference 8th American WaterJet Conference*, 1995.
[21] Morel Thomas. Experimental study of a jet-driven Helmholtz oscillator. *ASME Transactions-Journal of Fluids Engineering*, 1979, 101(3): 383-390.
[22] Jian Han, Tengfei Cai, Yan Pan, et al. Study on jet's characteristics of organ nozzle and Helmholtz nozzle. *Safety in Coal Mines*, 2017.
[23] Wenchuan Liu, Yong Kang, Mingxing Zhang, et al. Self-sustained oscillation and cavitation characteristics of a jet in a Helmholtz resonator. *International Journal of Heat and Fluid Flow*, 2017, 68: 158-172.
[24] Xiaochuan Wang, Yueqin Li, Yi Hu, et al. An experimental study on the jet pressure performance of Organ–Helmholtz (O-H), self-excited oscillating nozzles. *Energies*, 2020, 13(2): 367.
[25] H Man, K Yong, W Xiaochuan, et al. Experimental investigation on the rock erosion characteristics of a self-excited oscillation pulsed supercritical CO2 jet. *Applied Thermal Engineering*, 2018, 139: 445-455.
[26] Xiaolong Ding, Yong Kang, Deng Li, et al. Experimental investigation on surface quality processed by self-excited oscillation pulsed waterjet peening. *Materials*, 2017, 10(9): 989.
[27] J Fan, Z Wang, S Chen. Self-excited oscillation Frequency Characteristics of a Paralleled pulsed jet nozzle. *Energy Procedia*, 2017, 141: 619-624.
[28] W Liu, Y Kang, X Wang, et al. Integrated CFD-aided theoretical demonstration of cavitation modulation in self-sustained oscillating jets. *Applied Mathematical Modelling,* 2020, 79: 521-543.
[29] W Liu, Y Kang, M Zhang, et al. Frequency modulation and erosion performance of a self-resonating jet. *Applied Sciences-Basel*, 2017, 7(9): 932.
[30] Qiang Wu, Wei Wei, Bo Deng, et al. Dynamic characteristics of the cavitation clouds of submerged Helmholtz self-sustained oscillation jets from high-speed photography. *Journal of Mechanical Science and Technology*, 2019, 33(2): 621-630.
[31] Miao Yuan, Deng Li, Yong Kang, et al. The characteristics of self-resonating jet issuing from the Helmholtz nozzle combined with a venturi tube structure. *Journal of Applied Fluid Mechanics*, 2020, 13(3): 779-791.
[32] P Oshkai. Quantitative flow imaging approach to flow-acoustic coupling in pipeline-cavity systems. *Journal of Fluid Science and Technology*, 2014, 9: JFST0026-JFST0026.
[33] D Rockwell, J C Lin, P Oshkai, et al. Shallow cavity flow tone experiments: Onset of locked-on states. *Journal of Fluids and Structures*, 2003, 17(3): 381–414.
[34] Peng Wang, Yingzheng L. Intensified flow dynamics by second-order acoustic standing-wave mode: Vortex-excited acoustic resonances in channel branches. *Physics of Fluids*, 2019, 31(3).
[35] J E Rossiter. Wind tunnel experiments on the flow over rectangular cavities at subsonic and transonic speeds. *Aeron. Res. Counc*, 1966.